JACS
JOURNAL OF THE AMERICAN CHEMICAL SOCIETY
Article
pubs.acs.org/JACS

# Polyoxometalate-Based Cobalt–Phosphate Molecular Catalysts for Visible Light-Driven Water Oxidation

Xin-Bao Han,[†] Zhi-Ming Zhang,*[,†,‡,§] Teng Zhang,[‡] Yang-Guang Li,[†] Wenbin Lin,*[,‡,§] Wansheng You,[∥] Zhong-Min Su,[†] and En-Bo Wang*[,†]

[†]Key Laboratory of Polyoxometalate Science of the Ministry of Education, Faculty of Chemistry, Northeast Normal University, Changchun, Jilin 130024, P.R. China

[‡]Department of Chemistry, University of Chicago, 929 East 57th Street, Chicago, Illinois 60637, United States

[§]Collaborative Innovation Center of Chemistry for Energy Materials, College of Chemistry and Chemical Engineering, Xiamen University, Xiamen 361005, P.R. China

[∥]Institute of Chemistry for Functionalized Materials, Liaoning Normal University, Dalian, Liaoning 116029, P.R. China

Supporting Information

**ABSTRACT:** A series of all-inorganic, abundant-metal-based, high-nuclearity cobalt–phosphate (Co–Pi) molecular catalysts $[\{Co_4(OH)_3(PO_4)\}_4(SiW_9O_{34})_4]^{32-}$ (**1**), $[\{Co_4(OH)_3(PO_4)\}_4(GeW_9O_{34})_4]^{32-}$ (**2**), $[\{Co_4(OH)_3(PO_4)\}_4(PW_9O_{34})_4]^{28-}$ (**3**), and $[\{Co_4(OH)_3(PO_4)\}_4(AsW_9O_{34})_4]^{28-}$ (**4**) were synthesized and shown to be highly effective at photocatalytic water oxidation. The $\{Co_{16}(PO_4)_4\}$ cluster contains a $Co_4O_4$ cubane which is structurally analogous to the $[Mn_3CaO_4]$ core of the oxygen-evolving complex (OEC) in photosystem II (PSII). Compounds **1**–**4** were shown to be the first POM-based Co–Pi-cluster molecular catalysts for visible light-driven water oxidation, thus serving as a functional model of the OEC in PSII. The systematic synthesis of four isostructural analogues allowed for investigating the influence of different heteroatoms in the POM ligands on the photocatalytic activities of these Co–Pi cluster WOCs. Further, the POM-based photocatalysts readily recrystallized from the photocatalytic reaction systems with the polyoxoanion structures unchanged, which together with the laser flash photolysis, dynamic light-scattering, $^{31}P$ NMR, UV–vis absorption, POM extraction, and ICP-MS analysis results collectively confirmed that compounds **1**–**4** maintain their structural integrity under the photocatalytic conditions. This study provides not only a valuable molecular model of the "Co–Pi" catalysts with a well-defined structure but also an unprecedented opportunity to fine-tune high-nuclearity POM clusters for visible light-driven water splitting.

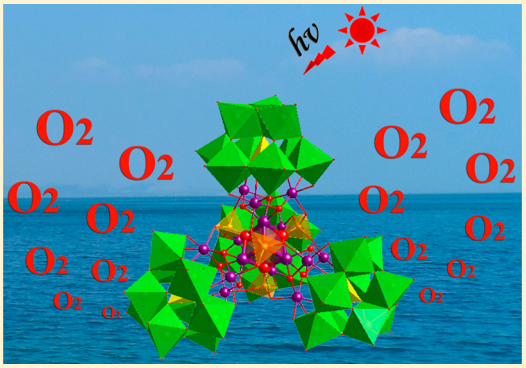


## INTRODUCTION

Sunlight provides abundant renewable energy source to meet mankind's future energy needs. Scientists have long been interested in developing photocatalysts for solar energy harvesting, transformation, and storage.[1−6] Water oxidation to dioxygen ($2H_2O \rightarrow 4H^+ + 4e^- + O_2$) is considered the critical step of the energy conversion scheme in both natural and artificial photosynthesis.[7−17] Co–Pi, an efficient heterogeneous oxygen-evolving catalyst, has been reported as possible structural and functional analogues to the $\{CaMn_4\}$ cubane in PSII.[8,18,19] To date, considerable progress has been made by depositing Co–Pi catalysts on various photoelectrodes including $\alpha$-$Fe_2O_3$, $BiVO_4$, Si, ZnO, and $WO_3$ to afford highly effective systems for water oxidation.[20−24] However, the structure of Co–Pi catalysts remains largely unknown as a result of the absence of detectable crystallites by X-ray diffraction.[8,25] The lack of detailed knowledge of the Co–Pi structures hinders the delineation of structure–property relationship which will aid in the further tuning of water oxidation activities. Recently, significant efforts have been devoted to exploring efficient, robust, and noble metal-free water-splitting catalysts that can mimic the functions of the $\{CaMn_4\}$ cubane in PSII,[26−28] and the progress in this field will provide an important opportunity for constructing molecular WOCs.[29,30]

Polyoxometalates (POMs), a class of metal–oxo clusters with oxygen-enriched surfaces,[31−34] provide robust all-inorganic ligand systems to encapsulate and protect active WOCs. The POMs can also undergo fast, reversible, and stepwise multielectron-transfer reactions without changing their structures. As a result, POMs have been explored as efficient functional components for constructing molecular photocatalysts.[35−39] For instance, lacunary POMs composed of W and Mo centers in the highest oxidation states[40−43] have been used as oxidatively resistant pure inorganic multidentate ligands

Received: December 18, 2013
Published: March 24, 2014

   dx.doi.org/10.1021/ja412886e | J. Am. Chem. Soc. 2014, 136, 5359−5366

in place of organic ligands for constructing well-defined structural models for photoredox processes.[44] In this area, the $\{Ru_4\}$ core embedded between two lacunary POM moieties has been proved to be promising all-inorganic candidates for WOCs,[44−47] and the single ruthenium substituted silico- and germanotungstates have recently been shown to be equally interesting targets.[48]

Given the extraordinarily large scale of solar energy utilization, intense research efforts have recently been devoted to mimicking photosynthesis with materials composed of earth-abundant elements. The first carbon-free, abundant-metal-based WOC $[Co_4(H_2O)_2(PW_9O_{34})_2]^{10-}$ was obtained by sandwiching a $\{Co_4\}$ cluster between two lacunary POM units, serving as an efficient WOC for chemical- and visible-light-induced water oxidation.[27,49] While this catalyst was reported to undergo decomposition to $CoO_x$ in the presence of a high positive potential bias,[50−52] it should be noted that the electrochemical water oxidation conditions used by Stracke et al. are different from the photocatalytic water oxidation conditions. Very recently, Hill et al. confirmed that the anion $[Co_4(H_2O)_2(PW_9O_{34})_2]^{10-}$ functions as the dominant molecular WOC, but not a precursor for $CoO_x$.[53] The crystal structure of a mixed-valence cobalt-containing polyoxoanion $[Co^{III}Co^{II}(H_2O)W_{11}O_{39}]^{7-}$ was very recently determined, which was reported to be an efficient and stable catalyst for $O_2$ production via visible light-driven water oxidation.[54] Sakai et al. explored two $Co^{III}$-containing polymolybdate WOCs $[CoMo_6O_{24}H_6]^{3-}$ and $[Co_2Mo_{10}O_{38}H_4]^{6-}$, and confirmed that the cobalt core is the $O_2$-evolving site in these two polyoxoanions.[55] Other Co-based POMs have also been reported, including Si-centered $[Co_4(H_2O)_2(SiW_9O_{34})_2]^{12-}$ and $[\{Co_4(\mu\text{-}OH)(H_2O)_3\}(Si_2W_{19}O_{70})]^{11-}$, but the latter was reported to be hydrolytically unstable.[56,57] Moreover, the $\{Co_9(H_2O)_6(OH)_3(HPO_4)_2(PW_9O_{34})_3\}^{16-}$ has been reported as a stable water oxidation electrocatalyst.[58]

We report here the synthesis, crystal structures, and photocatalytic water oxidation activities of four stable Co−Pi clusters: $[\{Co_4(OH)_3(PO_4)\}_4(SiW_9O_{34})_4]^{32-}$ (**1**), $[\{Co_4(OH)_3(PO_4)\}_4(GeW_9O_{34})_4]^{32-}$ (**2**), $[\{Co_4(OH)_3(PO_4)\}_4(PW_9O_{34})_4]^{28-}$ (**3**) and $[\{Co_4(OH)_3(PO_4)\}_4(AsW_9O_{34})_4]^{28-}$ (**4**). The hexadecanuclear Co−Pi cluster in these four compounds contains a $\{Co_4O_4\}$ cubane, which is analogous to the $[Mn_3CaO_4]$ cubane of the OEC in PSII. Compounds **1**−**4** are proved to be efficient visible light-driven Co−Pi WOCs with well-defined structures. Ge- and As-centers were introduced into the photoactive POM-based WOCs for the first time.[59] The systematic synthesis of four isostructural analogues allowed for investigating the influence of different heteroatoms of the POM ligands on the photocatalytic activities of these WOCs.

## EXPERIMENTAL SECTION

**Materials and Methods.** $[Ru(bpy)_3]Cl_2{\cdot}6H_2O$ and $Na_2S_2O_8$ were purchased from Aldrich. Other chemicals used for the syntheses were commercially purchased and used as received. $Na_{10}[\alpha\text{-}SiW_9O_{34}]{\cdot}18H_2O$, $Na_{10}[\alpha\text{-}GeW_9O_{34}]{\cdot}18H_2O$, $Na_9[\alpha\text{-}PW_9O_{34}]{\cdot}7H_2O$ and B−$Na_8[HAsW_9O_{34}]{\cdot}11H_2O$ were synthesized according to the literature,[60−62] and characterized by IR spectroscopy. Elemental analyses of Co, W, K, and Na were performed on a PLASMA-SPEC (I) inductively coupled plasma (ICP) atomic emission spectrometer. Thermogravimetric analyses were performed on a Perkin-Elmer TGA7 instrument in $N_2$ atmosphere with a heating rate of 5 °C·min$^{-1}$. IR spectra were recorded in the range of 400−4000 cm$^{-1}$ on an Alpha Centaurt FT-IR spectrophotometer with pressed KBr pellets. Nanosecond transient absorption measurements were performed with an Edinburgh Instruments LP920-laser flash photolysis spectrometer. The $^{31}P$ NMR spectra were obtained at 295 K in 5 mm o.d. tubes on a Bruker Ultra Shield 500 MHz spectrometer. The chemical shifts are given with respect to 85% $H_3PO_4$. Single-crystal data were collected on a Bruker Apex CCD diffractometer for **1**−**4** and a Rigaku R-AXIS RAPID IP diffractometer for **5**−**7** with graphite-monochromated Mo−K$\alpha$ radiation ($\lambda$ = 0.71073 Å). Suitable crystals were mounted in a thin glass tube and transferred to the goniostat. The structures of **1**−**7** were solved by the direct method and refined by the full-matrix least-squares fit on $F^2$ using the SHELXTL-97 crystallographic software package.[63]

**Synthesis of 1 and 2.** $CoCl_2{\cdot}6H_2O$ (0.78 g, 3.26 mmol) was dissolved in 40 mL of distilled water. $Na_{10}[\alpha\text{-}SiW_9O_{34}]{\cdot}18H_2O$ (1.18 g, 0.40 mmol) was added, and the mixture was stirred until a clear, purple solution was obtained. $Na_3PO_4{\cdot}12H_2O$ (0.60 g, 1.58 mmol) was then added, while a pH of 8.5−9.0 was maintained with 1.0 M KOH (aq). The resulting turbid solution was stirred for 3 h at room temperature, and the purple precipitate was removed by filtration. After that, 5 mL of 1.0 M KCl aqueous solution was added to the filtrate, which was stirred for another 30 min, and then filtered. The filtrate was kept in a 50 mL beaker to allow slow evaporation at room temperature. After one week, dark-purple crystals suitable for X-ray crystallography were obtained, washed with cold water, and air-dried to give 210 mg of **1** (17.0% yield). Anal. Calcd (%): K, 0.63; Na, 5.56; Co, 7.60; W, 53.3; Found: K, 0.55; Na, 5.64; Co, 7.69; W, 53.1. IR (KBr disks): 1626 (s), 1421 (m), 1137 (s), 1086 (m), 940 (s), 874 (m), 703 (s), 574 (w), 539 (w), 509 (w), 484 cm$^{-1}$ (w). The preparation of **2** (200 mg, 16.5% yield) is similar to that of **1**, except that 0.40 mmol $Na_{10}[\alpha\text{-}GeW_9O_{34}]{\cdot}18H_2O$ was used instead of $Na_{10}[\alpha\text{-}SiW_9O_{34}]{\cdot}18H_2O$ during the synthesis. Anal. Calcd (%) for **2**: K, 0.64; Na, 5.61; Co, 7.67; W, 53.8; Found: K, 0.56; Na, 5.72; Co, 7.55; W, 54.1. IR (KBr pellet) for **2**: $\tilde{U}$ = 1627 (s), 1469 (m), 1087 (s), 927 (m), 811 (m), 664 (m), 582 (w), 524 (w), and 459 cm$^{-1}$ (w).

**Synthesis of 3 and 4.** $CoCl_2{\cdot}6H_2O$ (0.78 g, 3.26 mmol) was dissolved in 40 mL of distilled water. $Na_9[\alpha\text{-}PW_9O_{34}]{\cdot}7H_2O$ (1.16 g, 0.40 mmol) was added and this mixture was stirred until a clear, purple solution was obtained. $Na_3PO_4{\cdot}12H_2O$ (0.60 g, 1.58 mmol) was then added while a pH of 8.3 − 9.0 was maintained with 1.0 M NaOH (aq). The resulting turbid solution was stirred for 3 h at room temperature and the purple precipitate was removed by filtration. After that, 5 mL of 1.0 M NaCl solution was added to the filtrate, which was stirred for another 30 min, and then filtered. The filtrate was kept in a 50 mL beaker to allow slow evaporation at room temperature. After one week, dark-purple crystals suitable for X-ray crystallography were obtained, washed with cold water, and air-dried to give 190 mg of **3** (16.1% yield). Anal. Calcd (%) for **3**: Na, 5.45; Co, 7.98; W, 56.0; Found: Na, 5.36; Co, 7.83; W, 55.8. IR (KBr pellet) for **3**: $\tilde{U}$ = 1629 (s), 1517 (m), 1426 (w), 1138 (s), 1091 (w), 1030 (m), 936 (m), 883 (m), 808 (w), 712 (s), and 480 cm$^{-1}$ (w); the preparation of **4** (72 mg, 6.1% yield) is similar to that of **3**, except that 0.40 mmol B−$Na_8[HAsW_9O_{34}]{\cdot}11H_2O$ was used instead of $Na_9[\alpha\text{-}PW_9O_{34}]{\cdot}7H_2O$ during the synthesis. Anal. Calcd (%) for **4**: Na, 5.26; Co, 7.71; W, 54.1; Found: Na, 5.33; Co, 7.85; W, 54.2. IR (KBr pellet) for **4**: $\tilde{U}$ = 1626 (s), 1092 (m), 1037 (w), 950 (m), 858 (w), 842 (w), 800 (m), 697 (m), 590 (m), 510 (w), 466 (w), and 438 cm$^{-1}$ (w).

**Visible Light-Driven Water Oxidation.** The photocatalytic water oxidation was carried out in an external illumination-type reaction vessel with a magnetic stirrer and analyzed by using an automatic $O_2$ monitoring system at room temperature. In the reaction vessel, different concentrations of **1**−**4** (0 − 30 $\mu$M) were dissolved in 20 mL of borate buffer solution (80 mM, pH 7.5−9.0), and $Na_2S_2O_8$ was used as a sacrificial electron acceptor. The reaction solution was first degassed by ultrasonication and added to the photosensitizer $[Ru(bpy)_3]Cl_2$ and then evacuated in the dark to ensure complete air removal. The photoirradiation was performed using a 300 W Xe lamp equipped with a long-pass filter (420 nm cutoff). The produced $O_2$ was analyzed by gas chromatography with a GC7890T instrument with a thermal conductivity detector and a 5 Å molecular sieve column (2 m × 3 mm) using Ar as carrier gas.


dx.doi.org/10.1021/ja412886e | J. Am. Chem. Soc. 2014, 136, 5359−5366

## RESULTS AND DISCUSSION

**Synthesis and Structures of 1−4.** Co−Pi catalysts are efficient oxygen-evolving complexes, but their structures remain largely unknown. In this work, lacunary POMs were employed as ideal oxidatively resistant, purely inorganic multidentate ligands to isolate Co−Pi clusters from condensing into amorphous solids (Figure 1). Room temperature reactions

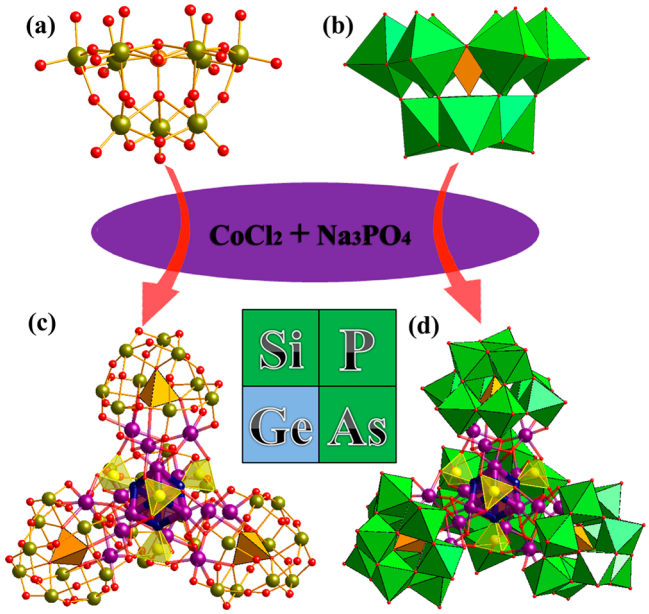


**Figure 1.** Synthetic route to obtain Co−Pi clusters **1**−**4**. Ball-and-stick (a) and polyhedral (b) representations of trivacant POMs: $[XW_9O_{34}]^{n-}$ (X = Si, Ge, $n$ = 10; X = P and As, $n$ = 9); (c) and (d) structure of polyoxoanions **1**−**4**. $WO_6$, green octahedra; $XO_4$ of trivacant POMs, orange tetrahedra; $PO_4$, yellow tetrahedra; O, red spheres; Co, violet spheres.

between four kinds of trivacant POMs, $[SiW_9O_{34}]^{10-}$, $[GeW_9O_{34}]^{10-}$, $[PW_9O_{34}]^{9-}$, or $[AsW_9O_{34}]^{9-}$ and $CoCl_2$ followed by the addition of $Na_3PO_4$ led to four stable Co−Pi clusters: $[\{Co_4(OH)_3PO_4\}_4(SiW_9O_{34})_4]^{32-}$ (**1**), $[\{Co_4(OH)_3PO_4\}_4(GeW_9O_{34})_4]^{32-}$ (**2**), $[\{Co_4(OH)_3PO_4\}_4(PW_9O_{34})_4]^{28-}$ (**3**) or $[\{Co_4(OH)_3PO_4\}_4(AsW_9O_{34})_4]^{28-}$ (**4**).

Compounds **1**−**4** are isostructural and crystallize in the cubic space group $Fd\bar{3}$. Single-crystal X-ray diffraction analyses revealed that compounds **1**−**4** all contain a high-nuclearity Co−Pi cluster $\{Co_{16}(PO_4)_4(OH)_{12}\}$ ($\{Co_{16}\}$) encapsulated by four $[XW_9O_{34}]^{n-}$ (X = Si, Ge, P, and As) units (Figures 1 and 2). Only the structure of **1** is discussed in detail here. In the asymmetric unit of **1**, there are two crystallographically independent cobalt ions Co1 and Co2 (Figures S1 and S2b, Supporting Information [SI]). They are both in a hexa-coordination environment. The coordination environment of Co1 is completed by three oxygen atoms from the lacunary POM units, two $\mu_3$-OH groups, and an $O_{Pi}$ atom, and the Co2 center is coordinated by three $\mu_3$-OH groups and three $O_{Pi}$ atoms.

The $\{Co_{16}\}$ cluster in compound **1** comprises a $\{Co_4O_4\}$ cubane unit in its center capped by four $\{Co_3\}$ units and four $PO_4$ ligands (Figure 2c and f). In the $\{Co_4O_4\}$ cubane, the Co−O distances fall into the range of 2.088(9)−2.137(7) Å in **1**, 2.114(13)−2.153(10) Å in **2**, 2.09(2)−2.144(16) Å in **3**, and 2.078(11)−2.164(10) Å in **4**, and the Co−Co distances are

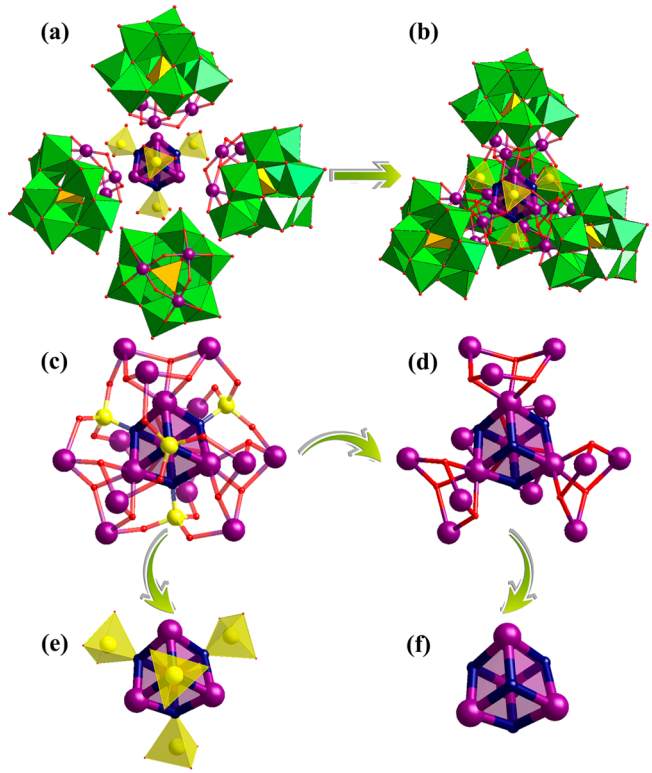


**Figure 2.** Polyhedral and ball-and-stick representations of the building blocks (a) and polyoxoanions (b) of **1**−**4**; ball-and-stick representation of $\{Co_{16}(OH)_{12}(PO_4)_4\}$ (c), $\{Co_{16}O_{16}\}$ (d), $\{Co_4(PO_4)_4\}$ (e), and $\{Co_4O_4\}$ (f) in **1**−**4**. $WO_6$, green octahedra; $XO_4$ of trivacant POMs, orange tetrahedra; $PO_4$, yellow tetrahedra; O, red spheres; Co, violet spheres.

3.222, 3.242, 3.205, and 3.247 Å, respectively. This structure is reminiscent of that of the $\{CaMn_4\}$ active site of the OEC in PSII. Further, the $\{Co_4O_4\}$ cubane was coordinated by four $PO_4$ ligands resulting in a $\{Co_4(PO_4)_4\}$ cluster (Figure 2e), which was connected with four $Co_3$ units via the $PO_4$ ligands and 12 $\mu_3$-OH groups, resulting in the high-nuclearity Co−Pi cluster $\{Co_{16}\}$. As shown in Figure S2c in SI, each $PO_4^{3-}$ ligand coordinated with six $Co^{2+}$ ions via its four O atoms in the Co−Pi cluster. Further, the high-nuclearity Co−Pi cluster was encapsulated by four trivacant POM ligands $[SiW_9O_{34}]^{10-}$ forming an assembly with the idealized $T_d$ symmetry. A previous study showed that the Co−Pi cluster-based tungstophosphate, which was also composed of a $\{Co_{16}\}$ cluster encapsulated by four trivacant POM ligands $[PW_9O_{34}]^{9-}$, exhibits interesting single-molecule magnet behivor.[64] All of the 16 cobalt ions in the $\{Co_{16}\}$ cluster exhibit a distorted octahedral coordination environment with Co−O bond lengths in the range 2.064(9)−2.332(10) Å. Bond valence sum (BVS) calculations indicated that all the cobalt ions are in the +2 oxidation state, which was supported by the X-ray photoelectron spectra of **1**−**4** (Figure S3, SI).

Alternatively, polyoxoanion **1** could be regarded as a tetramer composed of four $\{Co_4\}$-substituted $[\{Co_4(OH)_3(SiW_9O_{34})_4]$ units, which are fused together by four $PO_4$ ligands to result in the tetrameric polyoxotungstate cluster $[\{Co_4(OH)_3PO_4\}_4(SiW_9O_{34})_4]^{32-}$. In the $[\{Co_4(OH)_3(SiW_9O_{34})_4]$ unit, the trivacant POM unit $\{SiW_9O_{34}\}$, derived from the saturated Keggin structure by removal of three adjacent $WO_6$ octahedra, provides seven oxygen donor atoms that are capable of


dx.doi.org/10.1021/ja412886e | J. Am. Chem. Soc. 2014, 136, 5359−5366

coordinating with the $\{Co_4\}$ cluster (Figure S1, SI). As shown in Figure S2e in SI, three of the four $Co^{2+}$ ions in one Keggin unit substituted three $WO_6$ octahedra from three adjacent triplets to form a saturated Keggin structure. The fourth $Co^{2+}$ ion is linked to the Keggin anion by three $\mu_3$-OH atoms, which are all monoprotonated as identified by BVS calculations. It is worth mentioning that the high-nuclearity $\{Co_{16}\}$ cluster is well wrapped and separated by four $\{SiW_9O_{34}\}$ moieties, allowing the Co−Pi cluster to be well isolated to form a WOC without terminal atoms (such as $H_2O$ or Cl) coordinating to the central $Co^{2+}$ ions.

**Photocatalytic Water Oxidation by 1−4.** The photocatalytic water oxidation activities of compounds **1**−**4** were investigated in the borate buffer solution with $[Ru(bpy)_3]^{2+}$ as photosensitizer and $S_2O_8^{2-}$ as sacrificial electron acceptor. **1**−**4** were shown to catalyze water oxidation to produce $O_2$ under visible-light illumination as depicted in Scheme S1 in SI.[65,66] The photocatalytic water oxidation was investigated with different concentrations of **1**−**4** in 20 mL total volume, and their catalytic performances were compared as shown in Figure 3. The $O_2$ rapidly formed after 5 min of visible light

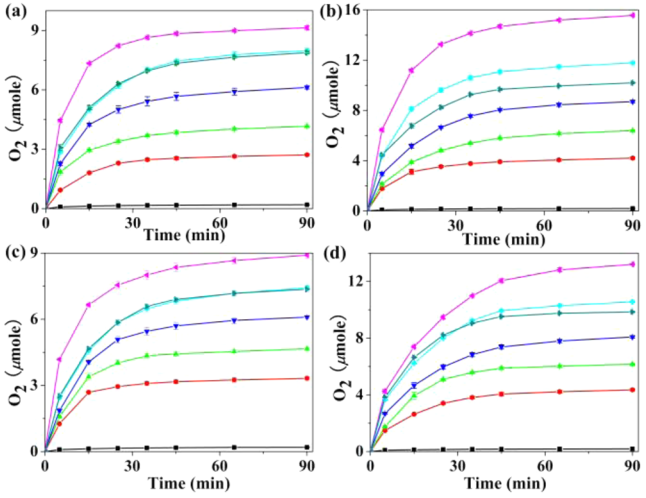


**Figure 3.** Kinetics of $O_2$ evolution in the photocatalytic system at different concentrations of (a) **1**; (b) **2**; (c) **3**; and (d) **4**. The symbols used to denote catalyst concentrations are: 0 $\mu$M (black ■), 3 $\mu$M (red •), 5 $\mu$M (lime green▲), 10 $\mu$M (royal blue▼), 15 $\mu$M (light blue diamond), 20 $\mu$M (magenta left-pointing triangle), and 30 $\mu$M (teal blue right-pointing triangle) (Error bar sd). Conditions: 300 W Xe lamp, 420−800 nm; 1.0 mM $[Ru(bpy)_3]Cl_2$, 5.0 mM $Na_2S_2O_8$, sodium borate buffer pH 9.0 (80 mM); total reaction volume 20 mL; vigorous stirring ($1.5 \times 10^3$ rpm).

illumination, and the $O_2$ evolution rate decreased over time. A maximum value of $O_2$ yield ($O_2$ yield = 2 × mole of $O_2$/mol of $Na_2S_2O_8$) (18.1% for **1**, 31.0% for **2**, 17.5% for **3**, and 26.4% for **4**) and $O_2$ evolution amount (9.0 $\mu$mol for **1**, 15.5 $\mu$mol for **2**, 8.7 $\mu$mol for **3**, and 13.2 $\mu$mol for **4**) were achieved for 0.4 $\mu$mol of **1**−**4** (20 $\mu$M) after 90 min illumination. The $O_2$ evolution amount corresponds to a turnover number (TON, defined as $n(O_2)/n$(catalyst)) of 22.5, 38.75, 20.25, and 33.0 for **1**−**4**, respectively (Figure S4, SI). Accordingly, it was found that the order of the maximum $O_2$ yield and $O_2$ evolution amount catalyzed by **1**−**4** are P-centered **3** ≤ Si-centered **1** < As-centered **4** < Ge-centered **2**. Also, the initial rate of water oxidation was consistent with the above sequence of the catalytic activity of these four catalysts. In 2011, Fukuzumi and co-workers reported that $[Ru^{III}(H_2O)GeW_{11}O_{39}]^{5-}$ POM exhibited a higher water oxidation catalytic activity than that of $[Ru^{III}(H_2O)SiW_{11}O_{39}]^{5-}$,[48] and a recent density functional theory study supported that the WOC activity of a Ge-centered mononuclear Ru POM catalyst is higher than that of the Si-centered analogue.[67] Further, we performed cyclic voltammetry (CV) of compounds **1** and **2**, which showed that **2** has a higher electrocatalytic water oxidation activity than **1**, and exhibits a slightly lower overpotential (the onset potential for **1** and **2** are ∼0.57 and ∼0.53 V, respectively) (Figure S5, SI). The $O_2$ yield increased with the catalyst concentrations increasing up to 20 $\mu$M and decreased with a higher catalyst concentration of 30 $\mu$M. However, the TON decreased from 44.5, 70.0, 54.2, and 71.5 to 22.5, 38.75, 20.25, and 33.0 for **1**−**4**, respectively, with their concentration increasing from 3 to 20 $\mu$M (Figure S4, SI). Moreover, an insoluble substance was observed after the catalytic reaction with 30 $\mu$M of **1**−**4**, which was not observed at low catalyst concentrations (≤20 $\mu$M). This phenomenon indicates the formation of ion-pairing salt precipitates, leading to the decrease of water oxidation activity of **1**−**4** at high catalyst concentrations.[54−56,68] We attempted to redissolve the POM−$Ru(bpy)_3$ salts in aqueous solutions, and DLS revealed the presence of particles of 263 and 336 nm in diameter for **1** and **3**, respectively (Figures S6 and S7, SI). Further, SEM images of the precipitates showed the existence of the nanoparticles of ∼100 nm and 150−250 nm in diameter for **1** and **3**, respectively (Figure S8, SI). EDX analyses of these nanoparticles indicated the presence of W, Ru, and Co (Figure S9, SI). These results argue against the formation of the cobalt oxide nanoparticle under the photocatalytic water oxidation conditions.

The photoinduced water oxidation was also investigated in the absence of **1**−**4**. $O_2$ evolution was detected with a maximum value of 0.19 $\mu$mol after 90 min irradiation, which corresponds to <2% of the amount of $O_2$ generated in the presence of **1**−**4**. In addition, there was no $O_2$ evolved without photosensitizer or $Na_2S_2O_8$. Further studies revealed that the pH value and concentrations of photosensitizer and sacrificial electron acceptor have important influences on the activity of the catalyst. Photocatalytic activities of **1** and **2** were explored by using 80 mM borate buffer with different pH values containing 20 $\mu$M catalysts, 1.0 mM $[Ru(bpy)_3]Cl_2{\cdot}6H_2O$, and 5.0 mM $Na_2S_2O_8$ (Figure 4). The $O_2$ evolution amount, $O_2$ yield, and TON increased from 3.9 $\mu$mol to 9.0 $\mu$mol, from 7.8% to 18.1%, and from 9.75 to 22.5 for **1** with the pH value increasing from 7.5 to 9.0. The $O_2$ evolution amount, $O_2$ yield,

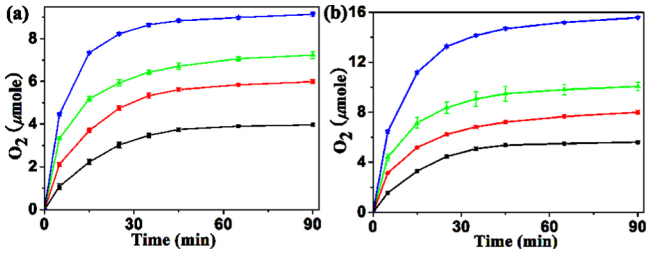


**Figure 4.** Kinetics of $O_2$ evolution of the photocatalytic system at different pHs of borate buffer (pH 7.5 (■); 8.0 (red •); 8.5 (lime green ▲); 9.0 (royal blue▼)) with 20 $\mu$M (a) **1** and (b) **2** (Error bar sd). Conditions: 300 W Xe lamp, 420−800 nm; 1.0 mM $[Ru(bpy)_3]Cl_2$, 5.0 mM $Na_2S_2O_8$, sodium borate buffer (80 mM); total reaction volume 20 mL; vigorous stirring ($1.5 \times 10^3$ rpm).


dx.doi.org/10.1021/ja412886e | J. Am. Chem. Soc. 2014, 136, 5359−5366

and TON increased from 5.5 $\mu$mol to 15.5 $\mu$mol, from 11.0% to 31.0%, and from 13.75 to 38.75 for **2** with the pH value increasing from 7.5 to 9.0. These results are consistent with fact that the water oxidation half reaction has a larger driving force at higher pHs. We also found that the photocatalytic water oxidation activity of **2** is higher than that of **1** in the same pH of 80 mM borate buffer.

**Kinetic Analysis of Photocatalytic Water Oxidation.** The photocatalytic water oxidation was also studied with different concentrations of photosensitizer and sacrificial electron acceptor (a and b of Figure 5). The amount of $O_2$

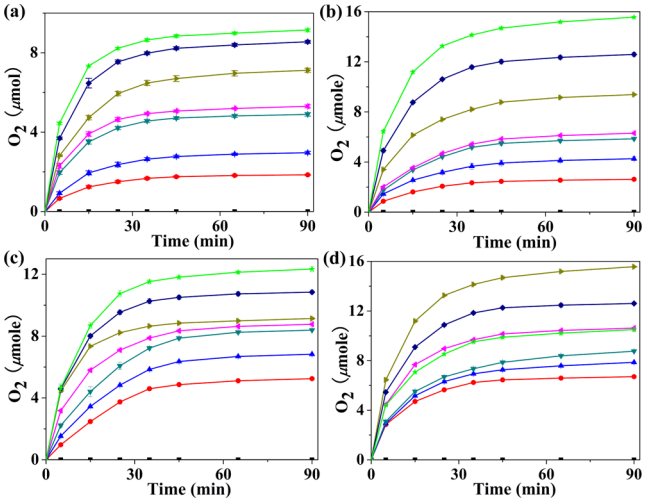


**Figure 5.** Kinetics of $O_2$ evolution of the photocatalytic system at different $[Ru(bpy)_3]^{2+}$ concentrations (0 mM (black ■); 0.1 mM (red •); 0.2 mM (royal blue ▲); 0.4 mM (teal blue▼); 0.5 mM (magenta left pointing triangle); 0.8 mM (olive green right pointing triangle); 0.9 mM (navy blue diamond); 1.0 mM (lime green star)) with 20 $\mu$M (a) **1** and (b) **2**, and at different $Na_2S_2O_8$ concentrations (0 mM, (■); 1.0 mM, (red •); 2.0 mM, (royal blue▲); 3.0 mM, (teal blue▼); 4.0 mM (magenta left pointing triangle); 5.0 mM (olive green right pointing triangle); 6.0 mM (navy blue diamond); 7.0 mM (lime green star)) with 20 $\mu$M (c) **1** and (d) **2** (Error bar sd). Conditions: Xe lamp, 420−800 nm; sodium borate buffer pH 9.0 (80 mM); total reaction volume 20 mL; vigorous stirring ($1.5 \times 10^3$ rpm).

evolution catalyzed by **1** and **2** both increased when the $[Ru(bpy)_3]Cl_2$ concentration increased from 0.1 mM to 1.0 mM. The $O_2$ yield increased from 3.78% to 18.1% for **1** and from 5.26% to 31.0% for **2**. The corresponding TON increases from 4.7 to 22.6 for **1** and from 6.58 to 38.75 for **2**. We also observed that the amount of $O_2$ evolution catalyzed by **2** is higher than that catalyzed by **1** in the same concentration of $[Ru(bpy)_3]Cl_2$. For compound **1**, the initial oxygen evolution rate shows linear dependence on the concentration of $[Ru(bpy)_3]^{2+}$ at a constant concentration of $S_2O_8^{2-}$ (Figure 6a). The initial oxygen evolution rate also shows linear dependence on the concentration of $S_2O_8^{2-}$ with its concentration lower than 5 mM and reaches saturation at the concentration of >5 mM. These experimental results indicate that the reaction is first order to both $[Ru(bpy)_3]^{2+}$ and $S_2O_8^{2-}$ (eq 1) at low $S_2O_8^{2-}$ concentrations. A rate constant $k$ of 9.16 $M^{-1}$ $min^{-1}$ was derived from linear fitting of initial oxygen evolution rates against $[Ru(bpy)_3]^{2+}$ concentrations.

$$\frac{d[O_2]}{dt} \approx k[Ru][S_2O_8^{2-}] \quad (1)$$

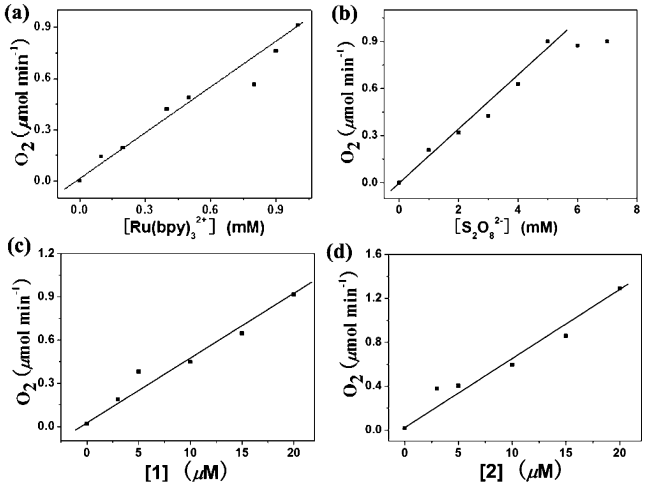


**Figure 6.** Initial $O_2$ evolution rate vs (a) $[Ru(bpy)_3^{2+}]$ ($[S_2O_8^{2-}]$ = 5 mM, [**1**] = 20 $\mu$M) and (b) $[S_2O_8^{2-}]$ ($[Ru(bpy)_3^{2+}]$ = 1 mM, [**1**] = 20 $\mu$M) for **1**; the initial $O_2$ evolution rate vs the concentrations of catalysts (c) **1** and (d) **2** ($[Ru(bpy)_3^{2+}]$ = 1 mM, $[S_2O_8^{2-}]$ = 5 mM). Conditions: Xe lamp, 420−800 nm; sodium borate buffer pH 9.0 (80 mM); total reaction volume 20 mL; vigorous stirring ($1.5 \times 10^3$ rpm).

However, the influence of $Na_2S_2O_8$ concentration on the photocatalytic water oxidation activity of compound **2** is different from that of **1**. The $O_2$ evolution amount decreased with the increasing concentration of $Na_2S_2O_8$ in the 5 −7 mM concentration range (Figure 5d), and the TON decreased from 38.75 to 26.75. A similar photocatalytic behavior is also observed for compound **4** (Figure S10, SI). As shown in Figure S10 in SI, the photocatalytic water oxidation reactions of compound **2** deviated from the first order in terms of $[Ru(bpy)_3]^{2+}$ or $S_2O_8^{2-}$ concentration, which indicates a highly complex process of photocatalytic water oxidation by **2**.[69] Parts c and d of Figure 6 show that initial oxygen evolution rates of **1** and **2** in the first 300 s are first order to the concentration of the catalysts with high $[Ru(bpy)_3]^{2+}$ and $S_2O_8^{2-}$ concentrations (relative to catalyst concentration).

As shown in Figure 3, $O_2$ quickly formed under visible-light illumination. An initial turnover frequency (TOF) in the first 300 s reached 0.053 $s^{-1}$ and 0.105 $s^{-1}$ for compounds **1** and **2**, respectively. Here the TOF for oxygen evolution is defined as $O_2$ evolution amount/catalyst amount/$\Delta t$, where $\Delta t$ is expressed in seconds. These TOF values are comparable to those of other Co-POM water oxidation catalysts.[53,55,57] For example, the two reported $Co^{II}$-based POMs with WOC activity, $[Co_4(H_2O)_2(PW_9O_{34})]^{10-}$ and $[\{Co_4(\mu\text{-}OH)\text{-}(H_2O)_3\}(Si_2W_{19}O_{70})]^{11-}$, have initial water oxidation TOF values of 0.08 $s^{-1}$ and 0.1 $s^{-1}$, respectively.[53,55,57] However, $[\{Co_4(\mu\text{-}OH)(H_2O)_3\}(Si_2W_{19}O_{70})]^{11-}$ is unstable and slowly undergoes hydrolysis in the catalytic process. For the $Co^{III}$-based POMs, a slightly higher initial TOF values of 0.11 $s^{-1}$ for $[CoMo_6O_{24}H_6]^{3-}$ and 0.16 $s^{-1}$ for $[Co_2Mo_{10}O_{38}H_4]^{6-}$ were achieved with 300 W Xe irradiation (400−800 nm).[55] Recently, a TOF of 0.5 $s^{-1}$ (in 60 s) was reported for a mixed-valence cobalt cluster-containing POM $[Co^{III}Co^{II}(H_2O)W_{11}O_{39}]^{7-}$.[54] To support these comparisons, we also determined the water oxidation catalytic activity of $[Co_4(H_2O)_2(PW_9O_{34})]^{10-}$ under our experimental conditions, which gave similar TOFs to those of the present Co-POMs (Figure S12a, SI).

**Reuse of 1−4.** The reuse of catalysts **1**−**4** was carried out by addition of another 5 mM of $Na_2S_2O_8$ to the reaction


dx.doi.org/10.1021/ja412886e | J. Am. Chem. Soc. 2014, 136, 5359−5366

solution after the first completion of catalytic experiment.[44,49,54] In the second run, the $O_2$ evolution amount decreased to 6.1, 9.1, 6.0, and 8.3 $\mu$mol for **1**−**4**, respectively (Figure S13, SI). DLS measurements showed the absence of any particles after the second run of photocatalytic water oxidation. In addition, after completion of the first run, 0.3−0.5 mM of the photosensitizer was added to reaction system together with another 5 mM of $Na_2S_2O_8$, and then photocatalytic water oxidation was run by the same operation as the first run. However, the $O_2$ evolution amount was similar to that of adding only 5 mM of $Na_2S_2O_8$ after the first run (Figure S13, SI). Further, the sodium borate buffer has a low buffer capacity at pH < 8.0. The pH after the photocatalytic experiments was determined and listed in Table S3 in SI. A significant drop of the pH value was observed for the photocatalytic system in sodium borate buffers with pH < 8. Also, we performed another second run of photocatalytic reaction by the addition of $Na_2B_4O_7$ to adjust the pH value of the reaction solution back to 9.0. The $O_2$ evolution amount was slightly higher than the red curve in Figure S13 in SI. These results indicate that the loss of the $O_2$ evolution activity after the first reaction run is influenced by a combination of several factors of the complicated solution environment after photocatalysis.

**The Stability Studies on 1−4.** Recently, the stability of molecular WOCs has received scrutiny as the WOCs might decompose into catalytically active oxide nanoparticles. POM-based WOCs can potentially have advantages because of the encapsulation and protection of active WOCs by the oxidatively stable POMs. In this work, we tested the stability of the Co−Pi clusters by laser flash photolysis and DLS measurements. Nanosecond laser flash photolysis experiments were carried out to measure the hole-transfer rates between the $[Ru(bpy)_3]^{3+}$ and the catalysts of **1**−**4**. The $[Ru(bpy)_3]^{3+}$ is *in situ* photogenerated in a few microseconds by irradiation of the solution containing 50 $\mu$M $[Ru(bpy)_3]^{2+}$ and 5.0 mM $S_2O_8^{2-}$ (Figure S14, SI) followed by hole scavenging by **1**−**4**. The black trace shows the constant $[Ru(bpy)_3]^{3+}$ concentration obtained in the absence of **1**−**4**, and the other traces display the obvious reduction of $[Ru(bpy)_3]^{3+}$ in the presence of **1**−**4** measured at different time intervals. The hole-scavenging activity of **1**−**4** remains constant with different aging times, revealing that **1**−**4** is stable over this time-scale.[70]

DLS measurements were performed in a solution of 20 $\mu$M **1** or **2**, $[Ru(bpy)_3]^{2+}$ (1 mM), $Na_2S_2O_8$ (5 mM) in 80 mM borate buffer (pH 9.0) after 90 min irradiation with a 300 W Xe lamp. The DLS results showed that no nanoparticles can be detected after photocatalytic water oxidation (Figures S15 and S16, SI). In addition, the same experiments were also conducted by using 10 $\mu$M $Co(NO_3)_2{\cdot}6H_2O$ instead of 20 $\mu$M **1** or **2** . After 15 min of irradiation, nanoparticles with a diameter of ∼147.7 nm were readily detected (Figure S17, SI). These results provide strong evidence that metal hydroxide/oxide nanoparticles (especially cobalt hydroxide/oxide nanoparticles) are not generated from the hydrolytic decomposition of **1** and **2** after the photocatalytic experiments.

$^{31}P$ NMR spectrum of compound **3** was taken to ascertain that the phosphate groups coordinate to the central $\{Co_{16}\}$ cluster in the borate buffer solution. Two $^{31}P$ peaks at ∼642 and 2156 ppm were observed (Figure S18, SI). These results indicate that phosphorus atoms exhibit two different chemical environments in the POM anions, which is consistent with the single-crystal structure.

Recently, Hill and co-workers devised an ingenious extraction method to address the molecular POM photocatalyst stability issue. POM species were extracted from the solution using tetraalkylammonium salts by taking advantage of the highly anionic nature of POMs, and the remaining soluble species could be easily quantified by elemental analysis.[53] We performed a similar study by using tetra-*n*-heptylammonium nitrate to extract the POM from the aqueous solution of the $Co_{16}$−POMs. After extraction of $Co_{16}$−POMs from solutions, inductively coupled plasma mass spectrometry (ICP-MS) was performed to quantify the amount of Co-containing species remaining in solution. Aging 20 $\mu$M of compounds **1**−**3** in 80 mM pH 9.0 sodium borate buffer for 3 h, followed by the extraction technique, yielded a concentration of cobalt at 0.65, 0.87, and 0.91 $\mu$M remaining in the reaction solution for compounds **1**, **2**, and **3**, respectively (Table S4, SI). The corresponding W concentrations are 1.46, 2.20, and 1.81 $\mu$M for these solutions, respectively. The POM extraction and ICP-MS analysis results thus indicated that less than <0.3% of POMs could have decomposed to release $Co^{2+}$ ions in the borate buffer. To rule out that the dissociated $Co^{2+}$ ions could be responsible for the observed photocatalytic water oxidation activity of **1**−**4**, we have performed the catalytic reaction with 1 $\mu$M $Co(NO_3)_2{\cdot}6H_2O$ under the same catalytic conditions. This experiment only produced a very small amount of $O_2$ (<6% of those produced by **1**−**4**).

For comparison, we also performed the photocatalytic water oxidation with 20 $\mu$M $Co(NO_3)_2{\cdot}6H_2O$ under the same conditions. As shown in Figure S12b in SI, compounds **1**−**4** exhibited higher catalytic activity than the control $Co^{2+}$ ions. Further, we performed the UV−vis spectra of compounds **1**−**4** in different pH values (7.5, 8.0, 8.5, and 9.0) with different aging times (0−90 min). As shown in Figures S19−S22 in SI, the UV−vis spectra remained unchanged with the time, supporting the stability of the POMs under these conditions.

These photocatalysts were also readily recrystallized from the photocatalytic systems with the polyoxoanion structures unchanged. After the photocatalytic experiment, the solution (with 20 $\mu$M catalysts) was kept at room temperature, and the solvent was allowed to slowly evaporate. After 2−3 weeks, single crystals suitable for X-ray crystallography recrystallized from the photocatalytic systems containing compounds **1**−**3**. These crystals have the formulas of $Na_{32}[\{Co_4(OH)_3PO_4\}_4(SiW_9O_{34})_4]{\cdot}52H_2O$ (**5**), $Na_{32}[\{Co_4(OH)_3PO_4\}_4(GeW_9O_{34})_4]{\cdot}114H_2O$ (**6**), and $Na_{28}[\{Co_4(OH)_3PO_4\}_4(PW_9O_{34})_4]{\cdot}58H_2O$ (**7**), respectively. Single-crystal X-ray diffraction analyses revealed that compounds **5** and **6** crystallized in the chiral space group *I*23 (flack parameters −0.02(3) and 0.26(8)), and compound **7** crystallized in the *Pbcn* space group (Table S2, SI). Although they crystallized in the different space groups from those of compounds **1**−**4**, polyoxoanions **5**−**7** also contained a high-nuclearity Co−Pi cluster $\{Co_{16}(PO_4)_4(OH)_{12}\}$ encapsulated by four trivacant $[XW_9O_{34}]^{n-}$ units, keeping the structural integrity of polyoxoanions in **1**−**3** (Figure S23, SI). In addition, the activity of photocatalytic water oxidation of the $\{Co_{16}\}$ compounds aged for 2 h and 48 h was the same as that of the fresh catalyst, which also provided additional evidence that compounds **1**−**4** were the molecular catalysts for the water oxidation reaction (Figure S24, SI).


dx.doi.org/10.1021/ja412886e | *J. Am. Chem. Soc.* 2014, 136, 5359−5366

## CONCLUSIONS

A series of carbon-free high-nuclearity Co−Pi clusters were synthesized and reported as the POM-based Co−Pi molecular photocatalysts. This study provides not only a valuable molecular model of the "Co−Pi" catalysts with a well-defined structure but also an unprecedented opportunity to fine-tune high-nuclearity POM clusters for visible light-driven water splitting. Their photocatalytic water oxidation activities have been systematically investigated and showed that **1**−**4** are all effective molecular catalysts and the photocatalytic performance is **3** ≤ **1** < **4** < **2** under visible light irradiation. As **1**−**4** are a series of Si-centered, Ge-centered, P-centered, and As-centered POMs with analogous structure, the comparison of the catalytic activity among **1**−**4** for water oxidation provides valuable insight into the influence of heteroatoms on oxygen evolution as well as the further design and synthesis of more stable and efficient WOCs. Multiple experiments collectively confirmed that compounds **1**−**4** are genuine molecular catalysts and maintain their structural integrity under the photocatalytic conditions.

## ASSOCIATED CONTENT

### Supporting Information

X-ray crystallography, supplementary structural figures, kinetic and EDX analysis, nanosecond laser flash photolysis experiments, DLS, $^{31}$P NMR spectra, EDX, UV−vis spectra, IR spectra, TG curves and CIF files. This material is available free of charge via the Internet at http://pubs.acs.org.

## AUTHOR INFORMATION

### Corresponding Authors

zhangzm178@nenu.edu.cn (Z.-M.Z.)
wenbinlin@uchicago.edu (W.L.)
wangeb889@nenu.edu.cn (E.-B.W.)

### Notes

The authors declare no competing financial interest.

## ACKNOWLEDGMENTS

This work was supported by the National Natural Science Foundation of China (21101022/91027002). We thank Dr. Cheng Wang for his valuable suggestions on kinetic analysis of photocatalytic $O_2$ evolution.

## REFERENCES

(1) Fujishima, A.; Honda, K. *Nature* **1972**, *238*, 37.
(2) Scholes, G. D.; Fleming, G. R.; Olaya-Castro, A.; Grondelle, R. V. *Nat. Chem.* **2011**, *3*, 763.
(3) Hochbaum, A. I.; Yang, P. D. *Chem. Rev.* **2010**, *110*, 527.
(4) Symes, M. D.; Cronin, L. *Nat. Chem.* **2013**, *5*, 403.
(5) Chen, X. B.; Li, C.; Grätzel, M.; Kosteckid, R.; Mao, S. S. *Chem. Soc. Rev.* **2012**, *41*, 7909.
(6) Wang, C.; deKrafft, K. E.; Lin, W. *J. Am. Chem. Soc.* **2012**, *134*, 7211.
(7) Umena, Y.; Kawakami, K.; Shen, J.-R.; Kamiya, N. *Nature* **2011**, *473*, 55.
(8) Kanan, M. W.; Nocera, D. G. *Science* **2008**, *321*, 1072.
(9) Toma, F. M.; Sartorel, A.; Iurlo, M.; Carraro, M.; Parisse, P.; Maccato, C.; Rapino, S.; Gonzalez, B. R.; Amenitsch, H.; Ros, T. D.; Casalis, L.; Goldoni, A.; Marcaccio, M.; Scorrano, G.; Scoles, G.; Paolucci, F.; Prato, M.; Bonchio, M. *Nat. Chem.* **2010**, *2*, 826.
(10) Duan, L. L.; Bozoglian, F.; Mandal, S.; Stewart, B.; Privalov, T.; Llobet, A.; Sun, L. C. *Nat. Chem.* **2012**, *4*, 418.
(11) Zou, Z. G.; Ye, J. H.; Sayama, K.; Arakawa, H. *Nature* **2001**, *414*, 625.
(12) Youngblood, W. J.; Lee, S.-H. A.; Kobayashi, Y.; Hernandez-Pagan, E. A.; Hoertz, P. G.; Moore, T. A.; Moore, A. L.; Gust, D.; Mallouk, T. E. *J. Am. Chem. Soc.* **2009**, *131*, 926.
(13) Kato, M.; Cardona, T.; Rutherford, A. W.; Reisner, E. *J. Am. Chem. Soc.* **2013**, *135*, 10610.
(14) Ellis, W. C.; McDaniel, N. D.; Bernhard, S.; Collins, T. J. *J. Am. Chem. Soc.* **2010**, *132*, 10990.
(15) Chen, H.; Faller, J. W.; Crabtree, R. H.; Brudvig, G. W. *J. Am. Chem. Soc.* **2004**, *126*, 7345.
(16) Hull, J. F.; Balcells, D.; Blakemore, J. D.; Incarvito, C. D.; Eisenstein, O.; Brudvig, G. W.; Crabtree, R. H. *J. Am. Chem. Soc.* **2009**, *131*, 8730.
(17) Wang, C.; Wang, J.-L.; Lin, W. *J. Am. Chem. Soc.* **2012**, *134*, 19895.
(18) Kanan, M. W.; Surendranath, Y.; Nocera, D. G. *Chem. Soc. Rev.* **2009**, *38*, 109.
(19) Reece, S. Y.; Hamel, J. A.; Sung, K.; Jarvi, T. D.; Esswein, A. J.; Pijpers, J. J. H.; Nocera, D. G. *Science* **2011**, *334*, 645.
(20) Zhong, D. K.; Sun, J. W.; Inumaru, H.; Gamelin, D. R. *J. Am. Chem. Soc.* **2009**, *131*, 6086.
(21) Pilli, S. K.; Furtak, T. E.; Brown, L. D.; Deutsch, T. G.; Turner, J. A.; Herring, A. M. *Energy Environ. Sci.* **2011**, *4*, 5028.
(22) Pijpers, J. J. H.; Winkler, M. T.; Surendranath, Y.; Buonassisi, T.; Nocera, D. G. *Proc. Natl. Acad. Sci. U.S.A.* **2011**, *108*, 10056.
(23) Steinmiller, E. M. P.; Choi, K.-S. *Proc. Natl. Acad. Sci. U.S.A.* **2009**, *106*, 20633.
(24) Seabold, J. A.; Choi, K.-S. *Chem. Mater.* **2011**, *23*, 1105.
(25) Du, P. W.; Kokhan, O.; Chapman, K. W.; Chupas, P. J.; Tiede, D. M. *J. Am. Chem. Soc.* **2012**, *134*, 11096.
(26) Dismukes, G. C.; Brimblecombe, R.; Felton, G. A. N.; Pryadun, R. S.; Sheats, J. E.; Spiccia, L.; Swiegers, G. F. *Acc. Chem. Res.* **2009**, *42*, 1935.
(27) Yin, Q. S.; Tan, J. M.; Besson, C.; Geletii, Y. V.; Musaev, D. G.; Kuznetsov, A. E.; Luo, Z.; Hardcastle, K. I.; Hill, C. L. *Science* **2010**, *328*, 342.
(28) Berardi, S.; Ganga, G. L.; Natali, M.; Bazzan, I.; Puntoriero, F.; Sartorel, A.; Scandola, F.; Campagna, S.; Bonchio, M. *J. Am. Chem. Soc.* **2012**, *134*, 11104.
(29) Yagi, M.; Kaneko, M. *Chem. Rev.* **2001**, *101*, 21.
(30) Sartorel, A.; Bonchio, M.; Campagna, S.; Scandola, F. *Chem. Soc. Rev.* **2013**, *42*, 2262.
(31) An, H. Y.; Wang, E. B.; Xiao, D. R.; Li, Y. G.; Su, Z. M.; Xu, L. *Angew. Chem., Int. Ed.* **2006**, *45*, 904.
(32) Zou, C.; Zhang, Z. J.; Xu, X.; Gong, Q. H.; Li, J.; Wu, C. D. *J. Am. Chem. Soc.* **2012**, *134*, 87.
(33) Izzet, G.; Ménand, M.; Matt, B.; Renaudineau, S.; Chamoreau, L.-M.; Sollogoub, M.; Proust, A. *Angew. Chem., Int. Ed.* **2012**, *51*, 487.
(34) Kikukawa, Y.; Kuroda, Y.; Yamaguchi, K.; Mizuno, N. *Angew. Chem., Int. Ed.* **2012**, *51*, 2434.
(35) Li, S. J.; Liu, S. M.; Liu, S. X.; Liu, Y. W.; Tang, Q.; Shi, Z.; Ouyang, S. X.; Ye, J. H. *J. Am. Chem. Soc.* **2012**, *134*, 19716.
(36) Huang, P.; Qin, C.; Su, Z. M.; Xing, Y.; Wang, X. L.; Shao, K. Z.; Lan, Y. Q.; Wang, E. B. *J. Am. Chem. Soc.* **2012**, *134*, 14004.
(37) Bernardini, G.; Wedd, A. G.; Zhao, C.; Bond, A. M. *Proc. Natl. Acad. Sci. U.S.A.* **2012**, *109*, 11552.
(38) Lü, J.; Lin, J. X.; Zhao, X. L.; Cao, R. *Chem. Commun.* **2012**, *48*, 669.
(39) Gao, J. K.; Cao, S. W.; Tay, Q. L.; Liu, Y.; Yu, L. M.; Ye, K. Q.; Mun, P. C. S.; Li, Y. X.; Rakesh, G.; Loo, S. C. J.; Chen, Z.; Zhao, Y.; Xue, C.; Zhang, Q. C. *Sci. Rep.* **2013**, *3*, 1853.
(40) Compain, J.-D.; Mialane, P.; Dolbecq, A.; Mbomekallé, I. M.; Marrot, J.; Sécheresse, F.; Rivière, E.; Rogez, G.; Wernsdorfer, W. *Angew. Chem., Int. Ed.* **2009**, *48*, 3077.
(41) Bassil, B. S.; Ibrahim, M.; Al-Oweini, R.; Asano, M.; Wang, Z. X.; Tol, J. V.; Dalal, N. S.; Choi, K.-Y.; Biboum, R. N.; Keita, B.; Nadjo, L.; Kortz, U. *Angew. Chem., Int. Ed.* **2011**, *50*, 5961.
(42) Mitchell, S. G.; Molina, P. I.; Khanra, S.; Miras, H. N.; Prescimone, A.; Cooper, G. J. T.; Winter, R. S.; Brechin, U. K.; Long, D. L.; Cogdell, R. J.; Cronin, L. *Angew. Chem., Int. Ed.* **2011**, *50*, 9154.

(43) Zhang, Z. M.; Yao, S.; Li, Y. G.; Wu, H. H.; Wang, Y. H.; Rouzières, M.; Clérac, R.; Su, Z. M.; Wang, E. B. *Chem. Commun.* **2013**, *49*, 2515.
(44) Geletii, Y. V.; Huang, Z. Q.; Hou, Y.; Musaev, D. G.; Lian, T. Q.; Hill, C. L. *J. Am. Chem. Soc.* **2009**, *131*, 7522.
(45) Geletii, Y. V.; Botar, B.; Kögerler, P.; Hillesheim, D. A.; Musaev, D. G.; Hill, C. L. *Angew. Chem., Int. Ed.* **2008**, *47*, 3896.
(46) Sartorel, A.; Carraro, M.; Scorrano, G.; Zorzi, R. D.; Geremia, S.; McDaniel, N. D.; Bernhard, S.; Bonchio, M. *J. Am. Chem. Soc.* **2008**, *130*, 5006.
(47) Besson, C.; Huang, Z.; Geletii, Y. V.; Lense, S.; Hardcastle, K. I.; Musaev, D. G.; Lian, T.; Proust, A.; Hill, C. L. *Chem.Commun.* **2010**, *46*, 2784.
(48) Murakami, M.; Hong, D. C.; Suenobu, T.; Yamaguchi, S.; Ogura, T.; Fukuzumi, S. *J. Am. Chem. Soc.* **2011**, *133*, 11605.
(49) Huang, Z. Q.; Luo, Z.; Geletii, Y. V.; Vickers, J. W.; Yin, Q. S.; Wu, D.; Hou, Y.; Ding, Y.; Song, J.; Musaev, D. G.; Hill, C. L.; Lian, T. Q. *J. Am. Chem. Soc.* **2011**, *133*, 2068.
(50) Stracke, J. J.; Finke, R. G. *J. Am. Chem. Soc.* **2011**, *133*, 14872.
(51) Stracke, J. J.; Finke, R. G. *ACS Catal.* **2013**, *3*, 1209.
(52) Stracke, J. J.; Finke, R. G. *ACS Catal.* **2014**, *4*, 79.
(53) Vickers, J. W.; Lv, H. J.; Sumliner, J. M.; Zhu, G. B.; Luo, Z.; Musaev, D. G.; Geletii, Y. V.; Hill, C. L. *J. Am. Chem. Soc.* **2013**, *135*, 14110.
(54) Song, F. Y.; Ding, Y.; Ma, B. C.; Wang, C. M.; Wang, Q.; Du, X. Q.; Fu, S.; Song, J. *Energy Environ. Sci.* **2013**, *6*, 1170.
(55) Tanaka, S.; Annaka, M.; Sakai, K. *Chem. Commun.* **2012**, *48*, 1653.
(56) Car, P.-E.; Guttentag, M.; Baldridge, K. K.; Alberto, R.; Patzke, G. R. *Green Chem.* **2012**, *14*, 1680.
(57) Zhu, G. B.; Geletii, Y. V.; Kögerler, P.; Schilder, H.; Song, J.; Lense, S.; Zhao, C. C.; Hardcastle, K. I.; Musaev, D. G.; Hill, C. L. *Dalton Trans.* **2012**, *41*, 2084.
(58) Goberna-Ferrón, S.; Vigara, L.; Soriano-López, J.; Galán-Mascarós, J. R. *Inorg. Chem.* **2012**, *51*, 11707.
(59) Lv, H. J.; Geletii, Y. V.; Zhao, C. C.; Vickers, J. W.; Zhu, G. B.; Luo, Z.; Song, J.; Lian, T. Q.; Musaev, D. G.; Hill, C. L. *Chem. Soc. Rev.* **2012**, *41*, 7572.
(60) Hervé, G.; Tézé, A. *Inorg. Chem.* **1977**, *16*, 2115.
(61) Ginsberg, A. P. *Inorg. Synth.* **1990**, *27*, 100.
(62) Bi, L. H.; Huang, R. D.; Peng, J.; Wang, E. B.; Wang, Y. H.; Hu, C. W. *J. Chem. Soc., Dalton Trans.* **2001**, 121.
(63) Sheldrick, G. M. *SHELXL97, Program for Crystal Structure Refinement*; University of Göttingen: Göttingen, Germany, 1997; Sheldrick, G. M. *SHELXS97, Program for Crystal Structure Solution*; University of Göttingen: Göttingen, Germany, 1997.
(64) Ibrahim, M.; Lan, Y. H.; Bassil, B. S.; Xiang, Y. X.; Suchopar, A.; Powell, A. K.; Kortz, U. *Angew. Chem., Int. Ed.* **2011**, *50*, 4708.
(65) Hara, M.; Waraksa, C. C.; Lean, J. T.; Lewis, B. A.; Mallouk, T. E. *J. Phys. Chem. A.* **2000**, *104*, 5275.
(66) Morris, N. D.; Mallouk, T. E. *J. Am. Chem. Soc.* **2002**, *124*, 11114.
(67) Lang, Z.-L.; Yang, G.-C.; Ma, N.-N.; Wen, S.-Z.; Yan, L.-K.; Guan, W.; Su, Z.-M. *Dalton Trans.* **2013**, *42*, 10617.
(68) Zhu, G. B.; Glass, E. N.; Zhao, C. C.; Lv, H. J.; Vickers, J. W.; Geletii, Y. V.; Musaev, D. G.; Song, J.; Hill, C. L. *Dalton Trans.* **2012**, *41*, 13043.
(69) Morris, N. D.; Suzuki, M.; Mallouk, T. E. *J. Phys. Chem. A.* **2004**, *108*, 9115.
(70) Natali, M.; Berardi, S.; Sartorel, A.; Bonchio, M.; Campagna, S.; Scandola, F. *Chem. Commun.* **2012**, *48*, 8808.